IUCrData

ISSN 2414-3146

(3*E*)-1,1,1-Trichloro-4-methoxy-4-phenylbut-3-en-2-one

Adriano Bof de Oliveira,[a]* Adailton João Bortoluzzi[b] and Alex Fabiani Claro Flores[a]

[a]Escola de Química e Alimentos, Universidade Federal do Rio Grande, Campus Carreiros, 96203-900 Rio Grande-RS, Brazil, and [b]Departamento de Química, Universidade Federal de Santa Catarina, Campus Universitário, 88035-972 Florianópolis-SC, Brazil. *Correspondence e-mail: adriano@furg.br

Received 27 November 2025
Accepted 4 December 2025

Edited by M. Bolte, Goethe-Universität Frankfurt, Germany

Keywords: crystal structure; alkenes isomerism; methoxyvinyl ketone.

CCDC reference: 2513465

Structural data: full structural data are available from iucrdata.iucr.org

The title compound, $C_{11}H_9Cl_3O_2$, (common name: β-aryl-β-methoxyvinyl trichloromethylketone) was crystallized from a chloroform solution at room temperature. The asymmetric unit comprises one molecule with all atoms in general positions and the *E* isomerism about the central vinyl entity could be undoubtedly determined. Weak intramolecular interactions between the ketone and the phenyl groups can be suggested, as two O···C distances [2.9154 (17) and 2.9780 (15) Å] are shorter than the van der Waals radii sum for the respective atoms (3.35 Å). As a result of the sp^3 C atoms and the C—C single bond between the phenyl ring and the central alkene fragment, the molecule is not planar. In the crystal, the molecules are linked by Cl···O weak interactions along the *a*-axis direction (2.962 Å intermolecular distances, compared to the 3.34 Å for the vdW radius sum) and these contacts were observed over the Hirshfeld surfaces set as d_{norm}, shape-index and curvedness modes. The Hirshfeld surface analysis mapped over the d_{norm} property indicates that four major contributions for the crystal cohesion are the H···Cl/Cl···H (34.2%), H···H (22.2%), H···C/C···H (13.5%) and H···O/O···H (10.6%) contacts. In addition, quantum-mechanical properties were calculated using the B3LYP/6–31 G(*d*,*p*) monomer wavefunctions model. The calculations were performed from a single molecular entity within a radial cluster of symmetry-generated molecules, with the *radius* set to 3.8 Å, and the total intermolecular energies between the molecular pairs range from −3.5 kJ/mol to −22.4 kJ mol^{-1}. An expanded structure section, set to 3 × 3 × 3 unit cells, was used for the visualization of the energy-framework (only the total energy property was selected and the energy cut-off was set to 10.0 kJ/mol). The synthesis and $^1H/^{13}C$ NMR data of the title compound are already published in the literature [Siqueira *et al.* (1994). *Quim. Nova*, **17**, 24–26].

3D view

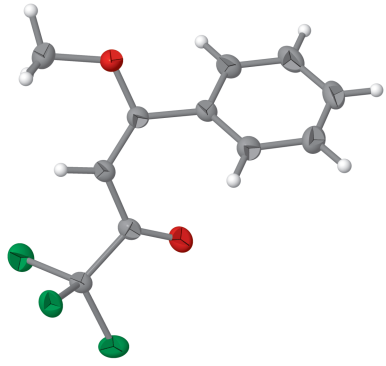

Chemical scheme

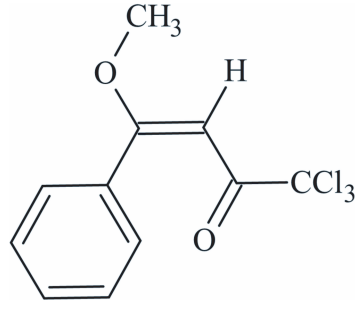

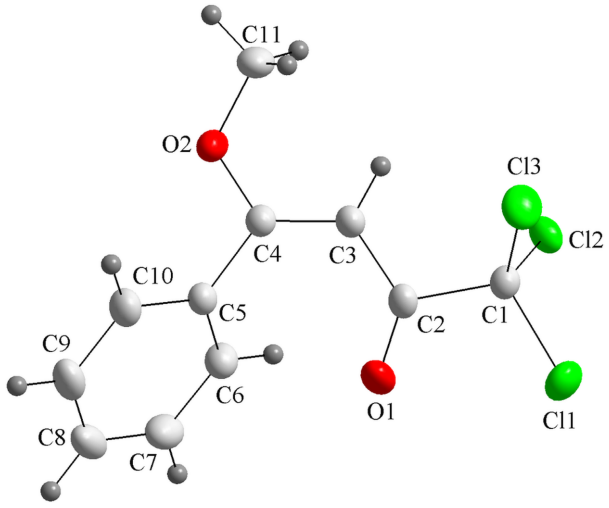

Figure 1
The molecular structure of the title compound, showing the atom labelling and displacement ellipsoids drawn at the 40% probability level.

Structure description

The title compound, *β*-aryl-*β*-methoxyvinyl trichloromethyl-ketone, belongs to the chemical class of alkoxyvinyl ketones, which are employed as starting materials or building blocks in heterocyclic chemistry (Druzhinin *et al.*, 2007; Martins *et al.*, 2008; Mittersteiner *et al.*, 2020; Nenajdenko *et al.*, 1997 & Vashchenko *et al.*, 2022). To the best of our knowledge, following a structural search with *SciFinder* (Chemical Abstracts Service, 2025), which returned over 50 results, the title compound was first obtained and characterized through ^{1}H and ^{13}C NMR spectroscopy by Siqueira *et al.* (1994).

Herein, as part of our interest in the chemical structure of reaction intermediates and educts for organic synthetic chemistry, we report the crystal structure and Hirshfeld analysis of the title alkoxyvinyl ketone derivative.

For the title compound, the asymmetric unit matches the molecular structure, with all atoms being located in general positions. The molecule is not planar due to the sp^3-hybridized C1 and C11 atoms and due to the single bond between the phenyl and the vinyl fragments, which allows a rotation around the axis through the C4—C5 atoms (Fig. 1), with the torsion angles for the C3—C4—C5—C6 and C3—C4—C5—C10 chains being −51.87 (18) and 131.55 (14)°, respectively. Concerning the C3—C4 vinyl entity, the *E* isomer could be indubitably determined. It is important to remark that the *E*/*Z* isomerism for some methoxyvinyl ketone derivatives, including natural products, is determined by kinetic and thermodynamic parameters, where the *Z* isomer is thermodynamically unstable and the *E* isomer is preferred (Kiuchi *et al.*, 1990).

In addition, intramolecular interactions for the title compound are observed. The distances between the O1 atom of the ketone group and the C5 and C6 atoms of the phenyl ring amount to 2.9780 (15) and 2.9154 (17) Å (Fig. 2), being shorter than the sum of the van der Waals radii for the respective atoms (3.35 Å; Batsanov, 2001; Rowland & Taylor, 1996).

In the crystal, the molecules are connected by weak intermolecular Cl···O interactions along [100] and build a one-dimensional supramolecular arrangement (Fig. 3). The Cl···O distances amount to 2.9620 (11) Å, while the sum of the vdW

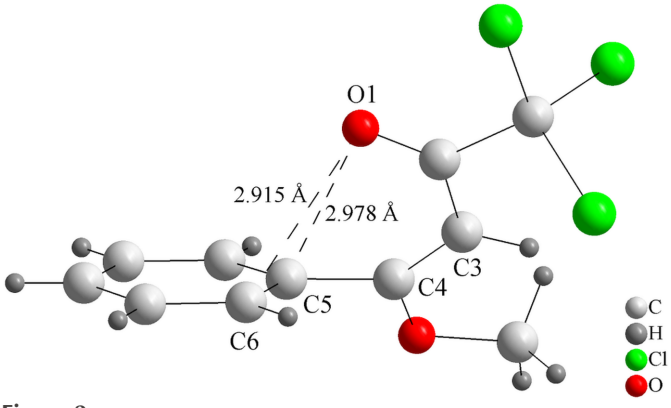

Figure 2
The molecular structure of the title compound showing the O1···C5 and O1···C6 intramolecular interactions. The interactions are drawn as dashed lines and the interatomic distances are indicated within the figure. This distances are shorter than the sum of the van der Waals radii for O and C (3.35 Å).

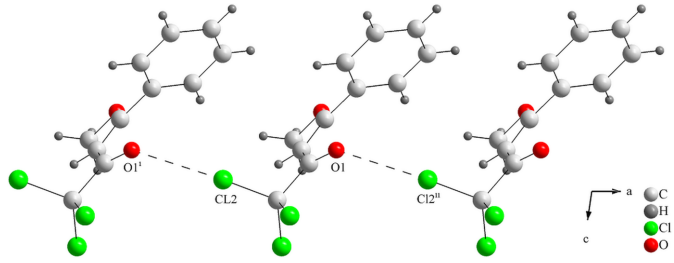

Figure 3
Part of the crystal structure of the title compound showing the O1···Cl2 intermolecular contacts as dashed lines. The O1···Cl2 distances amount to 2.9620 (11) Å and are shorter than the vdW radii sum for O and Cl atoms, which is 3.34 Å. [Symmetry codes: (i) $x-1, y, z$; (ii) $x+1, y, z$.]

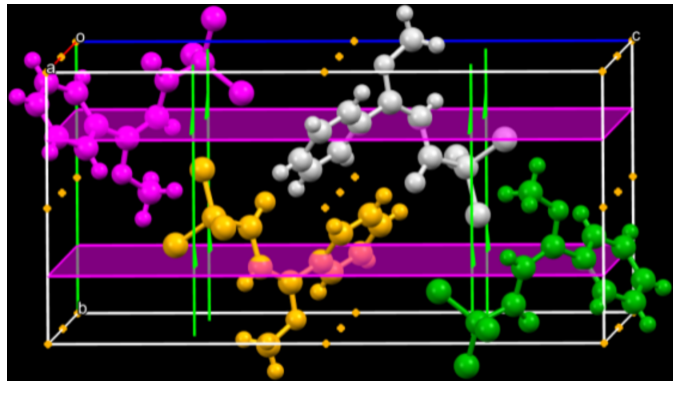

Figure 4
Graphical representation of the unit cell of the title compound. The molecules within the unit cell are colour-coded: grey for the asymmetric unit, yellow for the molecule generated through an inversion centre, green for the molecule generated through a twofold rotoinversion axis and pink for the molecule generated through a glide plane.

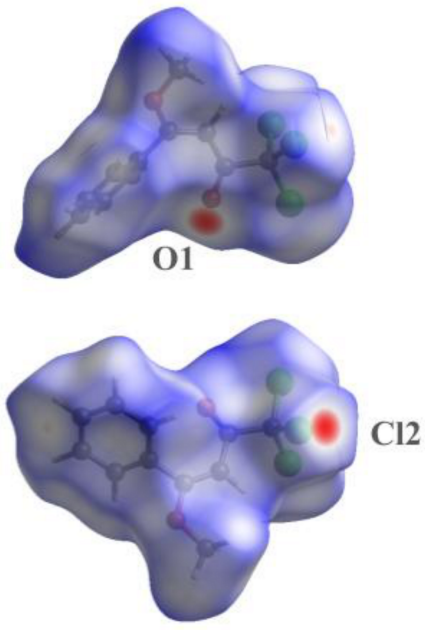

Figure 5
Two independent views for the graphical representation of the Hirshfeld surface of the title compound mapped over d_{norm}. The surfaces are drawn with transparency, the molecules are drawn using a ball-and-stick model and the regions with strongest intermolecular contacts are shown in red (corresponding to the O1 and Cl2 atom positions).

radii for the respective atoms is 3.34 Å (Batsanov, 2001; Rowland & Taylor, 1996). Otherwise, only very weak intermolecular interactions, *e.g.*, London dispersion forces can be presumed. There are four molecules in the unit cell and one graphical analysis with *Mercury 4.0* (Macrae *et al.*, 2020) reveals that all of them have their centres of gravity located on two glide planes. For a better understanding of the unit cell, a colour-coded system was used for the figure, as follows: the asymmetric unit was drawn in grey, the molecule generated through an inversion centre was drawn in yellow, the molecule generated through a twofold rotoinversion axis was drawn in green and the last one, generated by a glide plane, was drawn in pink (Fig. 4).

The Hirshfeld surface analysis (Hirshfeld, 1977), the graphical representations and the two-dimensional Hirshfeld surface fingerprints (HSFP) of the crystal structure were performed with *Crystal Explorer 21* (Spackman *et al.*, 2021). The first graphical representation of the Hirshfeld surface was set to the d_{norm} property and the regions with strongest intermolecular contacts, *i.e.*, the regions around the O1 and Cl2 atoms are indicated in red (Fig. 5). These atoms are those involved in the intermolecular interactions shown in Fig. 3. This analysis indicates that the four most relevant intermolecular interactions for crystal cohesion are the following: H···Cl/Cl···H (34.2%), H···H (22.2%), H···C/C···H (13.5%) and H···O/O···H (10.6%). The cited contributions to the crystal packing are shown as two-dimensional Hirshfeld surface fingerprint plots (HSFP) with cyan dots. Minor contributions to the crystal packing are the Cl···Cl (6.7%), C···Cl/Cl···C (5.7%) and Cl···O/O···Cl (5.5%), and are

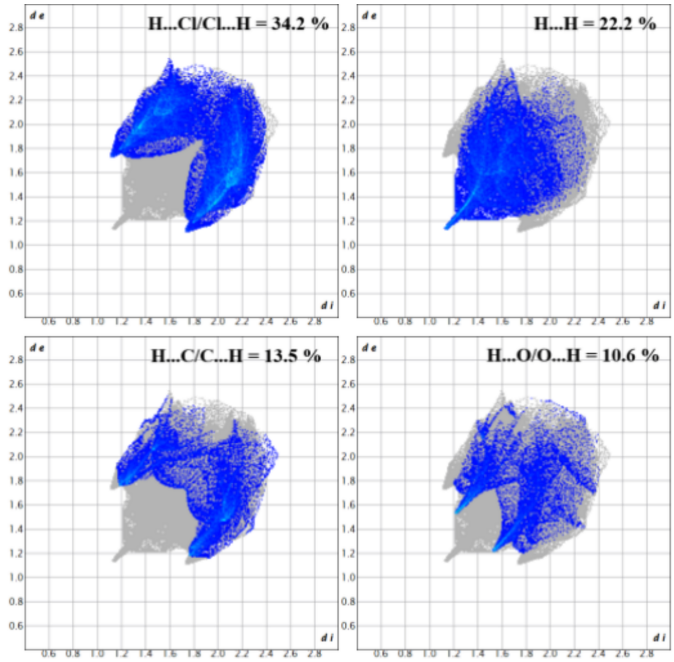

Figure 6
The Hirshfeld surface two-dimensional fingerprint plot (HSFP) for the title compound, showing the contacts in detail (cyan dots). The major contributions to the crystal cohesion are the following interactions: H···Cl/Cl···H (34.2%), H···H (22.2%), H···C/C···H (13.5%) and H···O/O···H (10.6%). All the minor contributions are not specified and drawn in grey. The d_i (*x*-axis) and the d_e (*y*-axis) values are the closest internal and external distances from given points on the Hirshfeld surface (in Å).

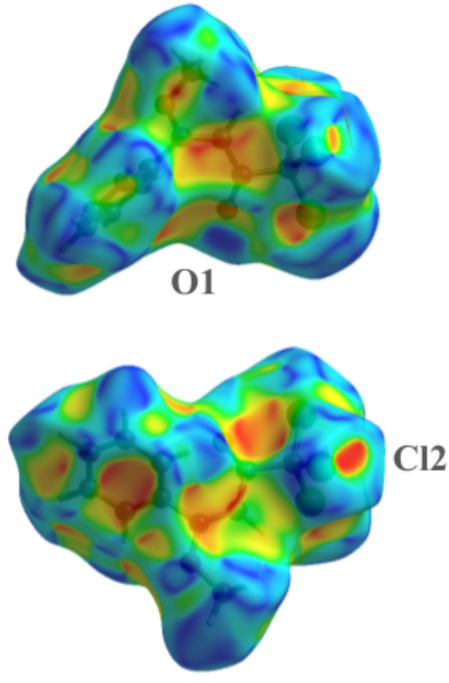

Figure 7
Two independent views for the graphical representation of the Hirshfeld surface of the title compound mapped over shape-index. The surfaces are drawn with transparency, the molecules are drawn using a ball-and-stick model and the regions with strongest intermolecular contacts are shown in dark red/concave (Cl2) and dark blue/convex (O1) colour/surface geometry.

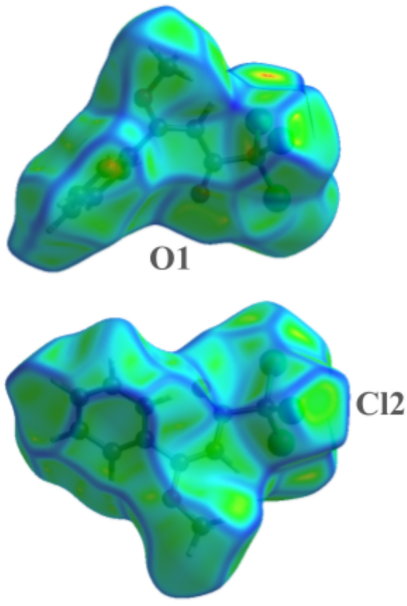

Figure 8
Two independent views for the graphical representation of the Hirshfeld surface of the title compound mapped over curvedness. The surfaces are drawn with transparency, the molecules are drawn using a ball-and-stick model and the locations suitable for intermolecular contacts are shown as flats regions, *e. g.*, the regions around the O1 and Cl2 atoms.

drawn in all graphics as grey dots (Fig. 6). The second graphical representation of the Hirshfeld surface was set to the shape-index property, in which the locations of the strongest intermolecular contacts are shown as concave red drawn surfaces, that indicate acceptor atoms, and convex blue drawn surfaces, that indicate the donor atoms involved in intermolecular interactions. For this surface analysis, the regions around the O1 and Cl2 atoms are the most important, geometrically (concave/convex) and by colour intensity (red/blue) (Fig. 7) and concur with the previous figures (Figs. 3 and 5). The last graphical representation of the Hirshfeld surface was set to the curvedness property. For this property, flat surface regions favour intermolecular contacts, while irregularities or vertices preclude short-range intermolecular forces. The surface regions around the O1 and Cl2 atoms are flat and proper to the intermolecular interactions between the molecules (Fig. 8) and this information agrees with the previous analysis and Figures (Figs. 3, 6 and 7). In contrast, the surface over the phenyl ring is irregular and shows vertices, which precludes intermolecular interactions, *e. g.*, the π-stacking with this entities. For details of the Hirshfeld surface properties, see: Spackman & Jayatilaka (2009).

The interaction energies between the molecules in the crystal structure were performed with the monomer wavefunctions B3LYP/6–31 G(*d*,*p*) model that is embedded in the *Crystal Explorer 21* (Spackman *et al.*, 2021). For the calculation of the energies, a radial cluster of 3.8 Å around the asymmetric unit was generated (Fig. 9). The total energy (E_{tot}) between pairs of molecules (N) rage from −3.5 to −22.4 kJ mol^{-1} and is a result of four energy components, *viz.* the electrostatic (E_{ele}, which ranges from −0.8 to −10.6 kJ mol^{-1}, polarization (E_{pol}, −0.2 to −2.9 kJ mol^{-1}) , dispersion (E_{dis},

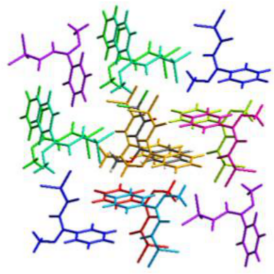

(a)

	N	Symop	R	Electron Density	E_ele	E_pol	E_dis	E_rep	E_tot
	1	-x, -y, -z	8.26	B3LYP/6-31G(d,p)	-5.5	-1.9	-23.8	10.9	-21.2
	2	x, y, z	6.27	B3LYP/6-31G(d,p)	-0.8	-1.9	-27.2	19.7	-13.8
	1	-x, -y, -z	6.62	B3LYP/6-31G(d,p)	-6.9	-1.7	-31.4	24.6	-20.7
	2	-x+1/2, y+1/2, -z+1/2	8.01	B3LYP/6-31G(d,p)	-6.7	-1.4	-18.8	18.8	-12.9
	2	-x+1/2, y+1/2, -z+1/2	6.67	B3LYP/6-31G(d,p)	-3.5	-1.4	-18.9	10.9	-14.5
	1	-x, -y, -z	10.29	B3LYP/6-31G(d,p)	-4.5	-0.8	-18.9	12.2	-14.4
	2	x, y, z	9.78	B3LYP/6-31G(d,p)	-3.4	-0.5	-3.1	0.5	-6.4
	2	x+1/2, -y+1/2, z+1/2	10.87	B3LYP/6-31G(d,p)	-1.0	-0.2	-7.3	6.6	-3.5
	1	-x, -y, -z	9.03	B3LYP/6-31G(d,p)	-10.6	-2.9	-18.6	11.7	-22.4

(b)

Figure 9
(*a*) Graphical representation of the radial cluster of 3.8 Å around the asymmetric unit, which lies in the centre of the picture and is drawn in black. The symmetry-generated molecules are colour-coded and the figure is simplified for clarity. (*b*) The box generated by *Crystal Explorer 21* (Spackman *et al.*, 2021) with the following data: the colour-codes of the molecule pairs (N), the symmetry operations (*Symop*), the distance between the molecular centroids (R, in Å) and the energy components (in kJ mol^{-1}).

−3.1 to −27.2 kJ mol^{-1}) , and exchange-repulsion (E_{dis}, 0.5 to 24.6 kJ mol^{-1} contributions. The number of molecule pairs (N), the symmetry operations for those (*Symop*), the distance between the molecular centroids (R; in Å) and the energy components (in kJ mol^{-1}) are given within the Figure. Finally, an energy framework for a crystal section of 3 × 3 × 3 unit cells was performed. The total energy of the section is drawn as cylinder mode in blue and set to 150 reference units. For the

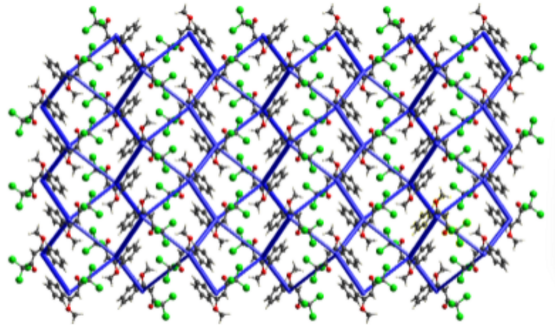

Figure 10
Graphical representation of the energy framework for a crystal section of 3 × 3 × 3 unit cells of the title compound viewed along [100]. The total energy is represented as cylinder mode in blue and set to 150 reference units. For clarity, the total energy cut-off was set to 10.0 kJ mol^{-1}.

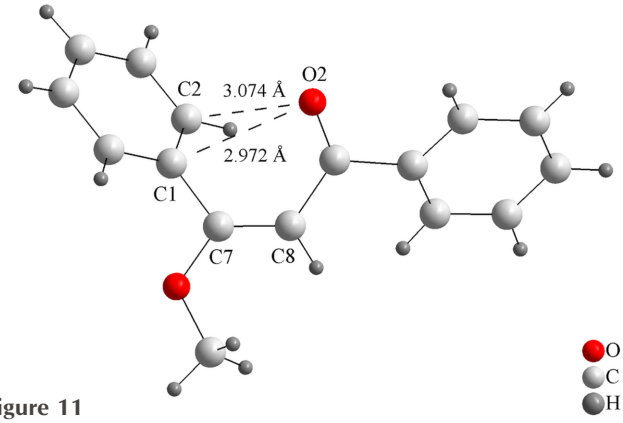

Figure 11
Molecular structure of a reference compound, the *E*-*β*-methoxychalcone derivative. As for the structure of the title compound, intramolecular interactions between the O2 atom of the ketone group and the C1 and C2 atoms of the phenyl ring are observed. The interactions are drawn as dashed lines and the interatomic distances are given within the figure (in Å), being shorter than the sum of the van der Waals radii for O and C (3.34 Å).

graphic, a total energy cut-off was set to 10 kJ mol^{-1} for clarity (Fig. 10). All the energy and symmetry parameters were based on the atomic coordinates and do not correspond to the centre of mass of the molecules (Mackenzie *et al.*, 2017; Spackman *et al.*, 2021).

From a database survey with the Cambridge Structural Database (CSD, accessed *via* WebCSD on November 23, 2025; Groom *et al.*, 2016) and the *CONQUEST* software (Version 2025.2.0, accessed on November 23, 2025; Bruno *et al.*, 2002), two similar compounds were selected for comparison with the title compound: *E*-*β*-methoxychalcone (CSD refode, SILFIC; No. 1259317) and *Z*-*β*-methoxychalcone (SILFEY; 1259316), both reported by Kiuchi *et al.* (1990).

In the asymmetric unit of the *E*-*β*-methoxychalcone derivative, intramolecular interactions between the ketone and the phenyl entities are observed (Fig. 11). The O2···C1 and O2···C2 distances amount to 2.972 Å and 3.074 Å, being shorter than the sum of the van der Waals radii for the respective atoms of 3.35 Å (Batsanov, 2001; Rowland & Taylor, 1996). The *E* isomer observed for the C7—C8 central vinyl fragment and the O···C intramolecular interactions are quite similar to those for the title compound (Fig. 2).

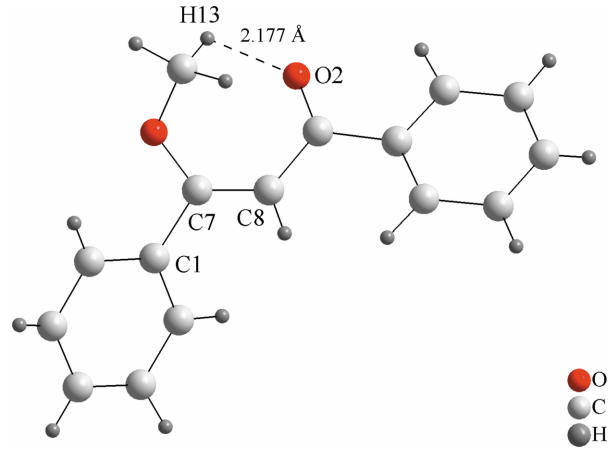

Figure 12
Molecular structure of a second reference compound, the *Z*-*β*-methoxychalcone derivative. For this isomer, an intramolecular interaction between the O2 atom of the ketone group and the H13 atom of the methyl fragment are observed. The interaction is drawn as a dashed linesand the interatomic distance is given within the figure (in Å), being shorter than the sum of the van der Waals radii for O and H (2.68 Å).

Table 1
Experimental details.

Crystal data	
Chemical formula	$C_{11}H_9Cl_3O_2$
M_r	279.53
Crystal system, space group	Monoclinic, $P2_1/n$
Temperature (K)	200
a, b, c (Å)	6.2726 (3), 9.7791 (4), 19.7780 (9)
β (°)	98.368 (1)
V (Å^3)	1200.27 (9)
Z	4
Radiation type	Mo $K\alpha$
μ (mm^{-1})	0.74
Crystal size (mm)	0.40 × 0.22 × 0.18
Data collection	
Diffractometer	Bruker APEXII CCD
Absorption correction	Multi-scan (Krause *et al.*, 2015)
T_{min}, T_{max}	0.704, 0.746
No. of measured, independent and observed [$I > 2\sigma(I)$] reflections	14717, 4368, 3767
R_{int}	0.015
(sin $\theta/\lambda)_{max}$ (Å^{-1})	0.758
Refinement	
$R[F^2 > 2\sigma(F^2)]$, $wR(F^2)$, S	0.033, 0.088, 1.07
No. of reflections	4368
No. of parameters	146
H-atom treatment	H-atom parameters constrained
$\Delta\rho_{max}$, $\Delta\rho_{min}$ (e Å^{-3})	0.43, −0.34

Computer programs: *APEX2* and *SAINT* (Bruker, 2014), *SHELXT2014/5* (Sheldrick, 2015*a*), *SHELXL2019/2* (Sheldrick, 2015*b*), *DIAMOND* (Brandenburg, 2006), *Crystal Explorer 21* (Spackman *et al.*, 2021), *Mercury* (Macrae *et al.*, 2020), *WinGX* (Farrugia, 2012), *publCIF* (Westrip, 2010) and *enCIFer* (Allen *et al.*, 2004).

For the *Z*-*β*-methoxychalcone derivative, an intramolecular interaction is observed between the ketone and the methyl entities (Fig. 12). The O2···H13 distance amounts to 2.177 Å, which is a value shorter then the van der Waals reference radii for the selected atoms of 2.68 Å (Batsanov, 2001; Rowland & Taylor, 1996). The *Z* isomer observed for the C7—C8 central vinyl fragment is thermodynamically unstable and tends to isomerize to the *E* isomer, as observed for natural *β*-methoxychalcone derivatives (Kiuchi *et al.*, 1990). As observed in the structure of the title compound, a rotation of the phenyl ring bonded to the central vinyl entity is possible due to the C—C simple bond between the two groups (C4—C5 for the title compound, Figs. 1–3; C1—C7 for the reference *E*/*Z*-*β*-methoxychalcone derivatives, Figs. 11 and 12).

Synthesis and crystallization

The synthesis of the title compound is already reported in the literature (Siqueira *et al.*, 1994). Colourless single crystals suitable for X-ray diffraction were obtained from a solution in chloroform at room temperature by slow evaporation of the solvent.

Refinement

Crystal data, data collection and structure refinement details are summarized in Table 1.

Acknowledgements

ABO is a former DAAD scholarship holder and *alumnus* of the University of Bonn, Germany, and thanks both of the institutions for the long-time support.

Funding information

Funding for this research was provided by: CAPES (Coordenação de Aperfeiçoamento de Pessoal de Nível Superior/Brazilian Federal Agency for Support and Evaluation of Graduate Education), from the Brazilian Federal Ministry of Education; CNPq (Conselho Nacional de Desenvolvimento Científico e Tecnológico/National Council for Scientific and Technological Development) and FINEP (Financiadora de Estudos e Projetos/Brazilian Innovation Agency), from the Brazilian Federal Ministry of Innovation, Science and Technology.

References

Allen, F. H., Johnson, O., Shields, G. P., Smith, B. R. & Towler, M. (2004). *J. Appl. Cryst.* **37**, 335–338.
Batsanov, S. S. (2001). *Inorg. Mater.* **37**, 871–885.
Brandenburg, K. (2006). *DIAMOND*. Crystal Impact GbR, Bonn, Germany.
Bruker (2014). *APEX2* and *SAINT*. Bruker AXS Inc., Madison, Wisconsin, USA.
Bruno, I. J., Cole, J. C., Edgington, P. R., Kessler, M., Macrae, C. F., McCabe, P., Pearson, J. & Taylor, R. (2002). *Acta Cryst.* B**58**, 389–397.
Chemical Abstracts Service (2025). Columbus, Ohio, USA (accessed *via* SciFinder on November 23, 2025).
Druzhinin, S. V., Balenkova, E. S. & Nenajdenko, V. G. (2007). *Tetrahedron* **63**, 7753–7808.
Farrugia, L. J. (2012). *J. Appl. Cryst.* **45**, 849–854.
Groom, C. R., Bruno, I. J., Lightfoot, M. P. & Ward, S. C. (2016). *Acta Cryst.* B**72**, 171–179.
Hirshfeld, H. L. (1977). *Theor. Chim. Acta* **44**, 129–138.
Kiuchi, F., Chen, X. & Tsuda, Y. (1990). *Chem. Pharm. Bull.* **38**, 1862–1871.
Krause, L., Herbst-Irmer, R., Sheldrick, G. M. & Stalke, D. (2015). *J. Appl. Cryst.* **48**, 3–10.
Mackenzie, C. F., Spackman, P. R., Jayatilaka, D. & Spackman, M. A. (2017). *IUCrJ* **4**, 575–587.
Macrae, C. F., Sovago, I., Cottrell, S. J., Galek, P. T. A., McCabe, P., Pidcock, E., Platings, M., Shields, G. P., Stevens, J. S., Towler, M. & Wood, P. A. (2020). *J. Appl. Cryst.* **53**, 226–235.
Martins, M. A. P., Moreira, D. N., Frizzo, C. P., Longhi, K., Zanatta, N. & Bonacorso, H. G. (2008). *J. Braz. Chem. Soc.* **19**, 1361–1368.
Mittersteiner, M., Bonacorso, H. G., Martins, M. A. P. & Zanatta, N. (2020). *Synthesis* **52**, 2008–2016.
Nenajdenko, V. G., Sanin, A. V. & Balenkova, E. S. (1997). *Molecules* **2**, 186–232.
Rowland, R. S. & Taylor, R. (1996). *J. Phys. Chem.* **100**, 7384–7391.
Sheldrick, G. M. (2015*a*). *Acta Cryst.* A**71**, 3–8.
Sheldrick, G. M. (2015*b*). *Acta Cryst.* C**71**, 3–8.
Siqueira, G. M., Flores, A. F. C., Clar, G., Zanatta, N. & Martins, M. A. P. (1994). *Quim. Nova* **17**(1), 24–26.
Spackman, M. A. & Jayatilaka, D. (2009). *CrystEngComm* **11**, 19–32.
Spackman, P. R., Turner, M. J., McKinnon, J. J., Wolff, S. K., Grimwood, D. J., Jayatilaka, D. & Spackman, M. A. (2021). *J. Appl. Cryst.* **54**, 1006–1011.
Vashchenko, B. V., Grygorenko, O. O. & Stepaniuk, O. O. (2022). *Ukr. Bioorg. Acta* **17**, 56–71.
Westrip, S. P. (2010). *J. Appl. Cryst.* **43**, 920–925.

full crystallographic data

IUCrData (2025). **10**, x251096 [https://doi.org/10.1107/S241431462501096X]

(3*E*)-1,1,1-Trichloro-4-methoxy-4-phenylbut-3-en-2-one

Adriano Bof de Oliveira, Adailton João Bortoluzzi and Alex Fabiani Claro Flores

(3*E*)-1,1,1-Trichloro-4-methoxy-4-phenylbut-3-en-2-one

Crystal data

$C_{11}H_9Cl_3O_2$
M_r = 279.53
Monoclinic, $P2_1/n$
a = 6.2726 (3) Å
b = 9.7791 (4) Å
c = 19.7780 (9) Å
β = 98.368 (1)°
V = 1200.27 (9) Å^3
Z = 4
$F(000)$ = 568
D_x = 1.547 Mg m^{-3}
Melting point = 358.15–359.15 K
Mo $K\alpha$ radiation, λ = 0.71073 Å
Cell parameters from 7757 reflections
θ = 3.0–32.6°
μ = 0.74 mm^{-1}
T = 200 K
Fragment, colourless
0.40 × 0.22 × 0.18 mm

Data collection

Bruker APEXII CCD diffractometer
Radiation source: fine-focus sealed X-ray tube, Bruker APEXII CCD diffractometer
Horizontally mounted graphite crystal monochromator
φ and ω scans
Absorption correction: multi-scan (Krause *et al.*, 2015)
T_{min} = 0.704, T_{max} = 0.746
14717 measured reflections
4368 independent reflections
3767 reflections with $I > 2\sigma(I)$
R_{int} = 0.015
θ_{max} = 32.6°, θ_{min} = 2.1°
h = −7→9
k = −14→10
l = −29→27

Refinement

Refinement on F^2
Least-squares matrix: full
$R[F^2 > 2\sigma(F^2)]$ = 0.033
$wR(F^2)$ = 0.088
S = 1.07
4368 reflections
146 parameters
0 restraints
Primary atom site location: structure-invariant direct methods
Secondary atom site location: difference Fourier map
Hydrogen site location: inferred from neighbouring sites
H-atom parameters constrained
$w = 1/[\sigma^2(F_o^2) + (0.0354P)^2 + 0.5708P]$ where $P = (F_o^2 + 2F_c^2)/3$
$(\Delta/\sigma)_{max}$ = 0.001
$\Delta\rho_{max}$ = 0.43 e Å^{-3}
$\Delta\rho_{min}$ = −0.34 e Å^{-3}

Special details

Geometry. All esds (except the esd in the dihedral angle between two l.s. planes) are estimated using the full covariance matrix. The cell esds are taken into account individually in the estimation of esds in distances, angles and torsion angles; correlations between esds in cell parameters are only used when they are defined by crystal symmetry. An approximate (isotropic) treatment of cell esds is used for estimating esds involving l.s. planes.

Refinement. Hydrogen atoms were located in a difference map and refined as riding on their parent atom with C_{methyl}—H = 0.98 Å and with $U(H)=1.5U_{eq}(C_{methyl})$ or with C—H = 0.95 Å and with $U(H)=1.2U_{eq}(C)$ for the remaining H atoms.

Fractional atomic coordinates and isotropic or equivalent isotropic displacement parameters (Å²)

	x	*y*	*z*	U_{iso}*/U_{eq}
C1	0.43349 (19)	0.41558 (12)	0.72330 (6)	0.0251 (2)
C2	0.56268 (18)	0.36450 (13)	0.66578 (6)	0.0247 (2)
C3	0.51636 (19)	0.22363 (13)	0.64522 (6)	0.0263 (2)
H3	0.414874	0.175059	0.667306	0.032*
C4	0.60816 (19)	0.15658 (12)	0.59660 (6)	0.0246 (2)
C5	0.74087 (19)	0.21757 (12)	0.54826 (6)	0.0247 (2)
C6	0.6678 (2)	0.32986 (14)	0.50812 (7)	0.0317 (3)
H6	0.532750	0.370289	0.512480	0.038*
C7	0.7922 (3)	0.38262 (15)	0.46180 (7)	0.0382 (3)
H7	0.741795	0.459059	0.434399	0.046*
C8	0.9898 (3)	0.32441 (16)	0.45525 (7)	0.0387 (3)
H8	1.075848	0.362076	0.424137	0.046*
C9	1.0613 (2)	0.21143 (17)	0.49412 (8)	0.0385 (3)
H9	1.195835	0.170859	0.489269	0.046*
C10	0.9366 (2)	0.15695 (15)	0.54035 (7)	0.0322 (3)
H10	0.985093	0.078485	0.566474	0.039*
C11	0.4704 (3)	−0.05854 (15)	0.62909 (8)	0.0388 (3)
H11A	0.534594	−0.045215	0.676845	0.058*
H11B	0.478284	−0.155469	0.617122	0.058*
H11C	0.319339	−0.029421	0.623042	0.058*
Cl1	0.50590 (7)	0.58393 (4)	0.74788 (2)	0.04314 (10)
Cl2	0.15408 (5)	0.40992 (3)	0.69129 (2)	0.03038 (8)
Cl3	0.48876 (6)	0.30748 (4)	0.79602 (2)	0.03966 (9)
O1	0.68633 (17)	0.44382 (11)	0.64506 (6)	0.0378 (2)
O2	0.58644 (17)	0.02147 (10)	0.58544 (5)	0.0331 (2)

Atomic displacement parameters (Å²)

	U^{11}	U^{22}	U^{33}	U^{12}	U^{13}	U^{23}
C1	0.0256 (5)	0.0257 (5)	0.0241 (5)	0.0021 (4)	0.0039 (4)	−0.0018 (4)
C2	0.0203 (4)	0.0284 (5)	0.0256 (5)	0.0021 (4)	0.0037 (4)	−0.0026 (4)
C3	0.0257 (5)	0.0260 (5)	0.0286 (5)	0.0002 (4)	0.0089 (4)	−0.0014 (4)
C4	0.0262 (5)	0.0239 (5)	0.0241 (5)	0.0018 (4)	0.0050 (4)	0.0005 (4)
C5	0.0264 (5)	0.0256 (5)	0.0227 (5)	0.0003 (4)	0.0061 (4)	−0.0017 (4)
C6	0.0381 (6)	0.0290 (6)	0.0292 (6)	0.0043 (5)	0.0094 (5)	0.0025 (5)
C7	0.0548 (9)	0.0325 (7)	0.0293 (6)	−0.0038 (6)	0.0125 (6)	0.0032 (5)
C8	0.0467 (8)	0.0417 (7)	0.0311 (6)	−0.0158 (6)	0.0173 (6)	−0.0087 (5)
C9	0.0306 (6)	0.0471 (8)	0.0407 (7)	−0.0043 (6)	0.0146 (5)	−0.0105 (6)
C10	0.0285 (6)	0.0349 (6)	0.0342 (6)	0.0039 (5)	0.0084 (5)	−0.0016 (5)
C11	0.0493 (8)	0.0279 (6)	0.0426 (7)	−0.0057 (6)	0.0184 (6)	0.0018 (5)
Cl1	0.0509 (2)	0.03137 (16)	0.0484 (2)	−0.00447 (14)	0.01142 (16)	−0.01452 (14)
Cl2	0.02343 (13)	0.03637 (16)	0.03254 (15)	0.00427 (11)	0.00811 (10)	0.00448 (11)

Cl3	0.0482 (2)	0.04573 (19)	0.02411 (14)	0.00755 (15)	0.00210 (12)	0.00613 (12)
O1	0.0345 (5)	0.0373 (5)	0.0452 (6)	−0.0106 (4)	0.0181 (4)	−0.0084 (4)
O2	0.0453 (5)	0.0237 (4)	0.0334 (5)	−0.0016 (4)	0.0164 (4)	−0.0019 (3)

Geometric parameters (Å, º)

C1—C2	1.5711 (16)	C6—H6	0.9500
C1—Cl1	1.7575 (12)	C7—C8	1.387 (2)
C1—Cl2	1.7755 (12)	C7—H7	0.9500
C1—Cl3	1.7780 (12)	C8—C9	1.383 (2)
C2—O1	1.2098 (15)	C8—H8	0.9500
C2—C3	1.4536 (17)	C9—C10	1.393 (2)
C3—C4	1.3593 (16)	C9—H9	0.9500
C3—H3	0.9500	C10—H10	0.9500
C4—O2	1.3432 (15)	C11—O2	1.4388 (17)
C4—C5	1.4814 (16)	C11—H11A	0.9800
C5—C10	1.3926 (17)	C11—H11B	0.9800
C5—C6	1.3930 (18)	C11—H11C	0.9800
C6—C7	1.3864 (19)		
C2—C1—Cl1	111.00 (8)	C5—C6—H6	120.0
C2—C1—Cl2	108.56 (8)	C6—C7—C8	120.36 (14)
Cl1—C1—Cl2	109.25 (6)	C6—C7—H7	119.8
C2—C1—Cl3	109.65 (8)	C8—C7—H7	119.8
Cl1—C1—Cl3	108.72 (6)	C9—C8—C7	119.86 (13)
Cl2—C1—Cl3	109.64 (7)	C9—C8—H8	120.1
O1—C2—C3	128.67 (11)	C7—C8—H8	120.1
O1—C2—C1	117.71 (11)	C8—C9—C10	120.20 (13)
C3—C2—C1	113.62 (10)	C8—C9—H9	119.9
C4—C3—C2	124.54 (11)	C10—C9—H9	119.9
C4—C3—H3	117.7	C9—C10—C5	119.96 (13)
C2—C3—H3	117.7	C9—C10—H10	120.0
O2—C4—C3	123.20 (11)	C5—C10—H10	120.0
O2—C4—C5	110.06 (10)	O2—C11—H11A	109.5
C3—C4—C5	126.73 (11)	O2—C11—H11B	109.5
C10—C5—C6	119.60 (12)	H11A—C11—H11B	109.5
C10—C5—C4	119.25 (11)	O2—C11—H11C	109.5
C6—C5—C4	121.06 (11)	H11A—C11—H11C	109.5
C7—C6—C5	119.98 (13)	H11B—C11—H11C	109.5
C7—C6—H6	120.0	C4—O2—C11	118.97 (10)
Cl1—C1—C2—O1	−1.68 (14)	O2—C4—C5—C6	127.31 (13)
Cl2—C1—C2—O1	118.42 (11)	C3—C4—C5—C6	−51.87 (18)
Cl3—C1—C2—O1	−121.83 (11)	C10—C5—C6—C7	−1.5 (2)
Cl1—C1—C2—C3	177.58 (8)	C4—C5—C6—C7	−178.10 (13)
Cl2—C1—C2—C3	−62.32 (11)	C5—C6—C7—C8	−0.2 (2)
Cl3—C1—C2—C3	57.44 (12)	C6—C7—C8—C9	1.3 (2)
O1—C2—C3—C4	−0.7 (2)	C7—C8—C9—C10	−0.7 (2)

C1—C2—C3—C4	−179.88 (11)	C8—C9—C10—C5	−1.0 (2)
C2—C3—C4—O2	170.12 (12)	C6—C5—C10—C9	2.1 (2)
C2—C3—C4—C5	−10.8 (2)	C4—C5—C10—C9	178.73 (12)
O2—C4—C5—C10	−49.27 (15)	C3—C4—O2—C11	−3.44 (19)
C3—C4—C5—C10	131.55 (14)	C5—C4—O2—C11	177.35 (12)